OSTEOPONTIN ISOFORMS: FUNCTIONAL HETEROGENEITY IN PROSTATE AND OVARIAN CARCINOMA

Tilli TM[1], Mello KD[1], Robbs BK[1], Wanderley JL[1], da Silva FR[1], Viola JP[1], Weber GF[2], Gimba ER[1,3]

[1]Programa de Medicina Experimental and Biologia Celular, Coordenação de Pesquisa – Instituto Nacional de Câncer (INCA), Programa de Pós Graduação Stricto Sensu em Oncologia do INCA, Rio de Janeiro-RJ, Brazil. [2]College of Pharmacy, University of Cincinnati, Cincinnati, Ohio, and [3]Departamento Interdisciplinar de Rio das Ostras-RIR, Polo Universitário de Rio das Ostras-Universidade Federal Fluminense (UFF), Rio das Ostras, Rio de Janeiro-RJ, Brazil

INTRODUCTION

Osteopontin (OPN) is a glycophosphoprotein overexpressed in various experimental models of malignancy and is involved in tumorigenesis and metastasis. OPN is recognized as a key prognostic marker during the ovarian carcinoma (OC) and prostate cancer (PCa) progression and is overexpressed in OC and PCa in relation to normal tissues. Alternative splicing of OPN leads to 3 splicing isoforms: osteopontin-a (OPNa), the full-length isoform; osteopontin-b (OPNb), which lacks exon 5 and osteopontin-c (OPNc), which presents deleted exon 4. However, the expression pattern and the roles of each of these isoforms have not been previously characterized in these tumor types.

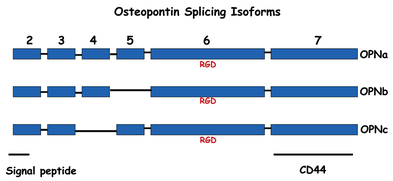

Figure 01. Structural features of the osteopontin splicing isoforms. The gene presents six translated exons. Osteopontin-a (OPNa) is the full-length isoform, while osteopontin-b (OPNb) lacks exon 5 and osteopontin-c (OPNc) lacks exon 4. The two main domains on the protein are separated by a protease-sensitive site. A N-terminal fragment encompasses the integrin-binding domains, while the CD44v-binding domain on the C-terminal part of the molecule. The integrin-binding site covers the sequence GRGDS. The scheme is not drawn to scale.

OBJECTIVES

Here we investigate the expression pattern of each OPN splicing isoform in ovarian and prostate tumor and non-tumor tissues. Based on OPN isoform expression profiling, we then investigated the functional roles of each one of them in ovarian and prostate cancer biology by using in vitro and *in vivo* models.

METHODOLOGY

- The expression pattern of each OPN splicing isoform was analyzed by quantitative real-time PCR in ovarian and prostate tumor and non-tumor tissues.
- The plasmid pCR3.1 constructs containing the human OPN splice variants were used to transfect OvCar-3 and PC-3 tumor cell lines. Transfections were performed using Lipofectamine™ 2000 (Invitrogen, CA). The functional roles of each OPN isoform was evaluated using *in vitro* e *in vivo* functional assays.

RESULTS

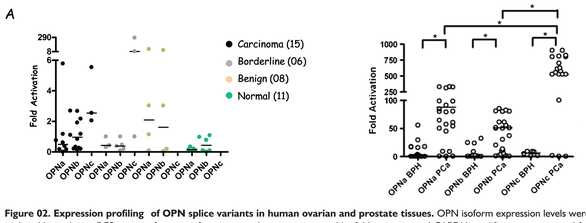

Figure 02. Expression profiling of OPN splice variants in human ovarian and prostate tissues. OPN isoform expression levels were analyzed by real time PCR using isoform specific primers and were represented by fold activation and GAPDH amplification as a control for template amount. (A) OPNa, OPNb and OPNc expression levels in different ovarian tissue samples, as represented by the legends on the right. Bars represent the median splice variant expression level. OPNc is only expressed in ovarian carcinoma and ovarian borderline tumor samples, while OPNa and OPNb are expressed in all ovarian tissues analyzed. (B) OPNa, OPNb and OPNc expression levels in different prostate tissue samples, as represented by the legends on the graph. Bars represent the median splice variant expression level. OPN isoforms are expressed both in tumor and benign tissues, although presenting higher expression levels in tumor tissues analyzed. Conversely, OPNc showed the higher expression level.

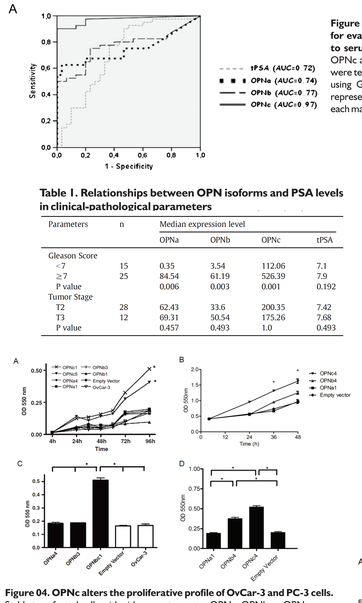

Table 1. Relationships between OPN isoforms and PSA levels in clinical-pathological parameters

Parameters	n	Median expression level			
		OPNa	OPNb	OPNc	tPSA
Gleason Score					
<7	15	0.35	3.54	112.06	7.1
≥7	25	84.54	61.19	526.39	7.9
P value		0.006	0.003	0.001	0.192
Tumor Stage					
T2	28	62.43	33.6	200.35	7.42
T3	12	69.31	50.54	175.26	7.68
P value		0.457	0.493	1.0	0.493

Figure 3. Receiver-operating characteristic (ROC) curves analyses for evaluating diagnostic properties of OPN isoforms as compared to serum PSA. Individual markers comprising tissue OPNa, OPNb and OPNc and serum PSA from men with PCa (n=40) and with BPH (n=30) were tested. OPN-SI expression levels were analyzed by qRT-PCR reaction using GAPDH as the internal control. Serum PSA was measured and represented as ng/mL on serum samples from these patients. The AUC for each marker are shown on the left with $p<0.05$.

Figure 04. OPNc alters the proliferative profile of OvCar-3 and PC-3 cells. Stably transfected cells with either empty vector, OPNa, OPNb or OPNc were plated. On every consecutive day, three wells per cell line were harvested and the total number of cells was measured. (A and B) Proliferation kinetics analysis was evaluated by crystal violet staining in OvCar-3 and PC-3 cells, respectively. OPNc present a higher proliferation rate as compared to OPNa, OPNb and empty vector. * $p < 0.05$ vs. empty vector control cells. (C and D) OPNc accelerates cell proliferation under reduced-serum conditions on both OvCar-3 and PC-3 cells. Cells were grown in 0.2% FBS and cell numbers were counted by crystal violet staining at 96 h after plating. O.D., optical density measured at +550 nm. * $p < 0.0001$ vs. empty vector control cells. (B and D) In PC-3 cells, OPNb presents intermediate proliferation behavior between OPNc and OPNa and controls.

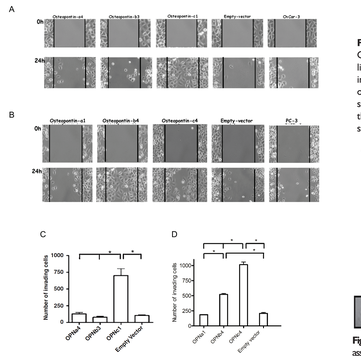

Figure 06. Roles of OPN isoforms on OvCar-3 and PC-3 cell migration and invasion. Cells overexpressing OPNa, OPNb and OPNc and transfected with empty-vector or OvCar-3 (A) and PC-3 (B) non-transfected cells, were plated and analyzed for cell migration by wound closure assay. The assays were conducted in the presence of mitomycin C, which suppresses the proliferation of rapidly growing cells. Phase-contrast micrographs photographs were taken at 0 and at 72hs after subjected to migration are shown. We represent here 24hs time point. Results were representative of 3 experiments. (C and D) Invading cells tested by transwell invasion assays were stained with crystal violet and the number of cells manually counted. Data are reported as average of number of invading cells ± S.D. of three independent experiments. $P < 0.001$.

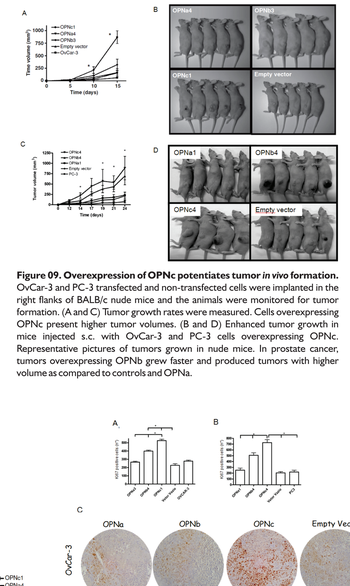

Figure 09. Overexpression of OPNc potentiates tumor *in vivo* formation. OvCar-3 and PC-3 transfected and non-transfected cells were implanted in the right flanks of BALB/c nude mice and the animals were monitored for tumor formation. (A and C) Tumor growth rates were measured. Cells overexpressing OPNc present higher tumor volumes. (B and D) Enhanced tumor growth in mice injected s.c. with OvCar-3 and PC-3 cells overexpressing OPNc. Representative pictures of tumors grown in nude mice. In prostate cancer, tumors overexpressing OPNb grew faster and produced tumors with higher volume as compared to controls and OPNa.

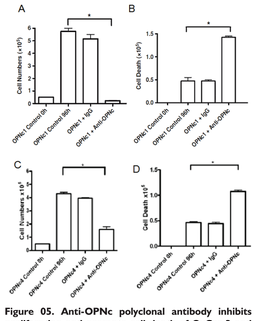

Figure 05. Anti-OPNc polyclonal antibody inhibits proliferation and promote cell death of OvCar-3 and PC-3 cells overexpressing OPNc *in vitro*. OvCar-3 and PC-3 overexpressing OPNc or non-transfected cells were treated with anti-OPNc antibody at the concentration of 4 µg/mL for 96 hs. Total number of cells (A and C) and cell death (B and D) were measured by Trypan blue. Significant differences are represented by asterisk. * $p < 0.0001$ vs. Osteopontin-c control 96 hs.

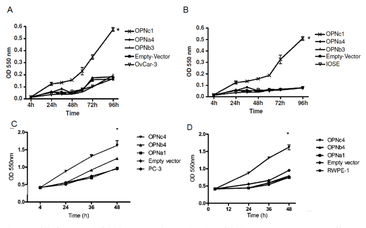

Figure 07. Secreted OPNc is mostly involved in OPNc pro-tumorigenic effects. OvCar-3 and PC-3 non transfected cells (A and C) and IOSE and RWPE-1 non tumor cell lines (B and D) were assayed for cell proliferation rates by crystal violet staining after incubation with conditioned medium from OPNa, OPNb, OPNc and empty vector overexpressing cells. In tumor, as well in non-tumoral ovarian and prostate cell lines secreted OPNc stimulates cell proliferation. All results are representative of at least three independent experiments. O.D., optical density measured at 550 nm. The standard deviations (error bars) indicate the variability within each experiment.

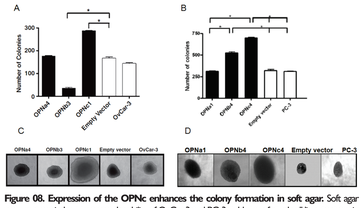

Figure 08. Expression of the OPNc enhances the colony formation in soft agar. Soft agar assay was carried out to assess the ability of OvCar-3 and PC-3 stably transfected cell lines to grow in an anchorage independent environment. Plates were examined microscopically for growth after 30 days. (A and B) Phase-contrast microscopy of representative OvCar-3 and PC-3 formed colonies. OvCar-3 and PC-3 cells overexpressing OPNa, OPNb and OPNc exhibited an increase in the size of colonies formed as compared to control cells. Pictures were obtained in 5X magnification. (C and D) Quantification of the number of OvCar-3 and PC-3 cell colonies grown in semisolid agarose medium transfected either with empty vector, OPNa, OPNb or OPNc expression vectors. When considering the number of colonies formed in OvCar-3 cells, OPNc behaved as an activator factor, while OPNb inhibited it. In PC-3 cells, cells overexpressing OPNc exhibited an increase in the number of colonies formed as compared to control cells. Additionally, PC-3 cells overexpressing OPNb presents intermediate behavior between OPNc and OPNa and controls.

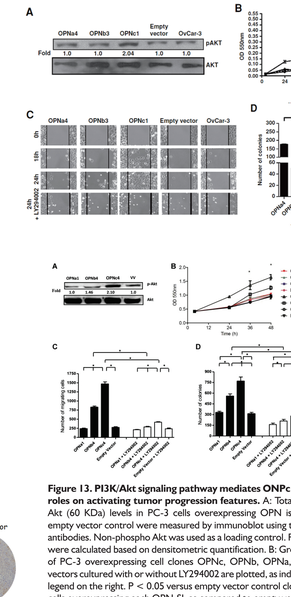

Figure 11. MMPs and VEGF are overexpressed in OvCar-3 and PC-3 cells overexpressing OPNb and OPNc isoforms. Induction of MMP2 (A and D), MMP9 (B and E), and VEGF (C and F) mRNA expression in xenograft tumors formed by cells overexpressing the three OPN isoforms, as compared to tumors formed by OvCar-3 and PC-3 cells transfected with empty vector controls. Total RNA from cells overexpressing OPNa, OPNb, OPNc, and empty vector control was prepared to conduct quantitative real-time PCR (qRT-PCR) analysis using glyceraldehyde 3-phosphate dehydrogenase (GAPDH) or actin as internal controls. The amount of targets was analyzed using the comparative CT method, where the threshold cycle (CT) values of each target sequence are given by the $2\Delta\Delta CT$ formula. We present the data as log n-fold change in gene expression normalized to the endogenous reference genes (GAPDH or actin) relative to the expression of cells overexpressing empty vector control. $P < 0.002$.

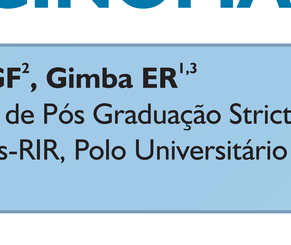

Figure 10. OPNc activates tumor formation by inducing proliferation. Tumors formed by each OPN isoforms OvCar-3 and PC-3 overexpressing cells, as well as empty vector were analyzed for Ki-67 positive staining. A and B: Quantification of immunohistochemical Ki-67 positive nuclei staining. C: Representative images of xenograft tumor spots showing Ki-67 expression as determined by nuclear staining, characterized by a dark brown reaction in the nucleus of tumor cells. 10X objectives on an Olympus BH-microscope.

Figure 13. PI3K/Akt signaling pathway mediates ONPc and OPNb roles on activating tumor progression features. A: Total Akt and p-Akt (60 KDa) levels in PC-3 cells overexpressing OPN isoforms and empty vector control were measured by immunoblot using their specific antibodies. Non-phospho Akt was used as a loading control. Fold changes were calculated based on densitometric quantification. B: Growth curves of PC-3 overexpressing cell clones OPNc, OPNb, OPNa, and empty vectors cultured with or without LY294002 are plotted, as indicated at the legend on the right. $P < 0.05$ versus empty vector control clone. C PC-3 cells overexpressing each OPN-SI, as compared to empty vector control were evaluated for cells migration capacity by transwell assays after LY294002 treatment at the 48 hr time point. D: The number colonies of anchorage independent growth formed by PC-3 cells overexpressing each OPN-SI as compared to empty vector control cells was analyzed in the presence or absence of LY294002 inhibitor. $P < 0.002$.

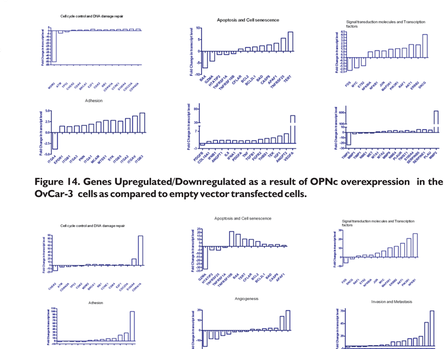

Figure 14. Genes Upregulated/Downregulated as a result of OPNc overexpression in the OvCar-3 cells as compared to empty vector transfected cells.

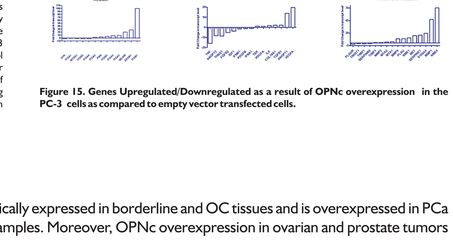

Figure 15. Genes Upregulated/Downregulated as a result of OPNc overexpression in the PC-3 cells as compared to empty vector transfected cells.

Figure 12. PI3K/Akt signaling pathway mediates ONPc roles on activating tumor progression features. A - PI3K/Akt signaling is activated in OvCar-3 cells overexpressing OPNc. Total Akt and p-Akt levels in OvCar-3 cells overexpressing OPNa, OPNb, OPNc, and empty vector control were measured using Western blotting using their specific antibodies. Non phospho Akt were used as a loading control. Fold changes were calculated based on densitometric quantification; B - OPNc-induced OvCar-3 cell proliferation is specifically blocked by the PI3K inhibitor. Growth curves of OvCar-3 overexpressing clones and non-transfected OvCar-3 cells cultured with or without PI3K LY294002 inhibitor are plotted. LY294002 was added 4 hours after cell plating and culture media maintained for all proliferation kinetics as measured by crystal violet assay. * $P < 0.0001$ vs. empty vector control clone; C - OPNc-induced OvCar-3 cell migration is blocked by the PI3K inhibitor. OvCar-3 cells were seeded, and migration capacity was evaluated after carrying out streaks in wound closure assay. LY294002 inhibitor was added just after carrying out the streaks and cell migration was analyzed at the 24 hour time point; D - OPNc overcomes LY294002 effects on inhibiting the number of OvCar-3 cells colonies formed in soft agar. Colonies were cultured in soft agar in the presence or absence of LY294002 inhibitor added to culture medium, which was changed every 3 days until reaching 30 days of culture. * $P < 0,002$.

CONCLUSIONS

- This work describes that OPNc is specifically expressed in borderline and OC tissues and is overexpressed in PCa tumors as compared to prostate BPH samples. Moreover, OPNc overexpression in ovarian and prostate tumors could be an additional information that could help to better understand OC and PCa tumorigenesis and the specific genetic modifications related to this process.
- Notably, the stimulating actions of OPNc overexpression on events associated with tumoral progression denotes its important role on ovarian and prostate cancer tumorigenesis and progression. Altogether, these results provide compelling evidence that OPNc could be used not only as additional biomarker to better diagnose in OC and PCa, but also as an indicative marker of ovarian and prostate cancer progression.
- Functional effects specifically observed for OPNc in favoring OC and PCa growth and progression are probably related to the absence of amino acids 32-58 contained on exon 4. PCR gene expression array data demonstrated that OPNc isoform significantly modulates the expression of several genes involved in fundamental cancer signaling pathways in both tumor models. Our data indicate that OC and PCa cells overexpressing OPNc and its increased proliferation behavior is mediated by the PI3-K signaling pathway. According to these data, we suggest that deregulated alternative splicing of OPN transcripts may potentially contribute to the pathophysiology of OC and PCa progression and that OPNc isoform act as an OC and PCa maintenance gene.
- A better understanding of the specific behavior of OPNc isoform and its corresponding gene expression control may lead to therapeutic strategies that selectively downregulate OPNc altering its pro-tumorigenic properties

Supported by: CAPES, SWISS BRIDGE FOUNDATION, FAPERJ, CNPq, Ministério da Saúde/FAF, INCT do Câncer

Projeto Gráfico: Serviço de Edição e Informação Técnico-Científica / INCA